Quantum Hall Effect in Hydrogenated Graphene

J. Guillemette, S. S. Sabri, Binxin Wu, K. Bennaceur, P. E. Gaskell, M. Savard, P. L. Lévesque, F. Mahvash, A. Guermoune, M. Siaj, R. Martel, T. Szkopek, and G. Gervais

Quantum Hall Effect in Hydrogenated Graphene

J. Guillemette[1,2], S.S. Sabri[2], B. Wu[1], K. Bennaceur[1], P.E. Gaskell[2], M. Savard[1], P.L. Lévesque[3],
F. Mahvash[2,4], A. Guermoune[2,4], M. Siaj[4], R. Martel[3], T. Szkopek[2], and G. Gervais[1]⋆

[1] *Department of Physics, McGill University, Montréal, QC, H3A 2T8, Canada*
[2] *Department of Electrical and Computer Engineering,*
McGill University, Montréal, QC, H3A 2A7, Canada
[3] *Department of Chemistry, Université de Montréal, Montréal, QC H3C 3J7, Canada*
[4] *Department of Chemistry, Université du Québec à Montréal, Montréal, QC, H3C 3P8, Canada and*
⋆*corresponding author: gervais@physics.mcgill.ca*

The quantum Hall effect is observed in a two-dimensional electron gas formed in millimeter-scale hydrogenated graphene, with a mobility less than 10 cm^2/V · s and corresponding Ioffe-Regel disorder parameter $(k_F\lambda)^{-1} \gg 1$. In zero magnetic field and low temperatures, the hydrogenated graphene is insulating with a two-point resistance of order of $250h/e^2$. Application of a strong magnetic field generates a negative colossal magnetoresistance, with the two-point resistance saturating within 0.5% of $h/2e^2$ at 45T. Our observations are consistent with the opening of an impurity-induced gap in the density of states of graphene. The interplay between electron localization by defect scattering and magnetic confinement in two-dimensional atomic crystals is discussed.

Two-dimensional atomic crystals have attracted much attention as surfaces with unique low-dimensional electron transport behaviour, most notably the zero-gap semiconductor graphene [1]. The relativistic Dirac dispersion of electrons in graphene leads to an anomalous four-fold degenerate quantum Hall (QH) sequence [2–5]. Common to these studies is low disorder, with a mean free path λ large compared to electron Fermi wavelength $\lambda_F = 2\pi/k_F$, with the cleanest graphene samples exhibiting the fractional quantum Hall (FQH) effect [6, 7]. We report here our discovery of a quantum Hall effect in graphene at the opposite extreme, whereby hydrogenation was used to induce a short mean-free path beyond the Ioffe-Regel limit $k_F\lambda \sim 1$ for the onset of strongly insulating behaviour. Our work illustrates the importance of the interplay between electron localization by point defect scattering and magnetic confinement in two-dimensional atomic crystals.

We present experimental results on electronic transport in graphene where neutral point defects are introduced by hydrogenation. Previous electron transport studies of hydrogenated graphene were interpreted as evidence for graphane[8], a two-dimensional polymer of carbon and hydrogen. More recently, angle resolved photoemission spectroscopy (ARPES) [9] and scanning tunneling microscopy (STM) [10] measurements have demonstrated the opening of a gap in the density of states of hydrogenated graphene. The object of our work is to probe the magnetotransport properties of hydrogenated graphene. We focus on large area (millimeter-scale) graphene that was exposed to an atomic hydrogen beam resulting in insulating behaviour ($dR/dT < 0$ at zero magnetic field) and a low-temperature resistance $R \sim 250 \times h/e^2$ far above the Ioffe-Regel limit for the onset of insulating behaviour. Application of a 45 T magnetic field induces a transition to a well formed quantum Hall state with a two point resistance $R_{2pt} = h/2e^2$ accurate to within 0.5%. The insulator-quantum Hall transition coincides with the magnetic length (ℓ_B) approaching, and becoming less than the mean defect spacing inferred from Raman spectroscopy (λ_D).

Disordered graphene samples were prepared from pristine, large-area, monolayer graphene samples grown by chemical vapour deposition (CVD) on Cu foils [11], with growth details reported elsewhere [12]. Graphene monolayers were transferred to oxidized silicon wafers and electrically contacted for electron transport experiments. Disorder was controllably introduced into the graphene by exposure to a beam of atomic hydrogen produced by thermally cracking molecular hydrogen with a white-hot tungsten capillary [13]. The room temperature two-point resistance R_{2pt} of graphene samples was monitored versus atomic hydrogen exposure *in situ* in an ultra-high vacuum chamber, Fig.1. The room temperature resistance of graphene devices was observed to increase with exposure to atomic hydrogen, as has been observed in graphene exposed to hydrogen plasma [8]. Atomic hydrogen exposure produces an exponential growth in resistance, and a corresponding exponential shortening of carrier mean-free path λ. The Ioffe-Regel disorder parameter $(k_F\lambda)^{-1} \simeq (M/2) \cdot (e^2/h) \cdot R_{2pt}$, where $M = 4$ accounts for spin and valley degeneracy, is consequently significantly increased beyond the limit for the onset of strongly insulating behaviour.

The disorder introduced by hydrogenation was observed by Raman spectroscopy, Fig. 2**A**. The Raman Stokes peaks G and G' associated with pristine sp^2 carbon indicate clean, monolayer CVD graphene prior to hydrogenation (blue spectrum). The emergence of strong disorder-induced peaks D and D' upon hydrogenation
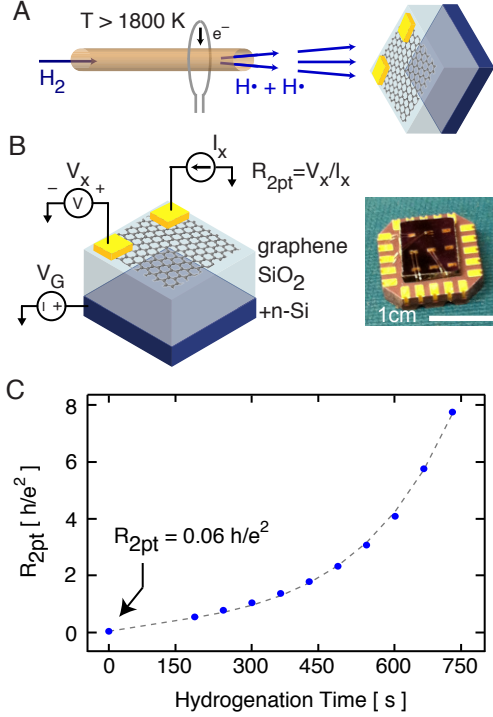
FIG. 1. Schematic of graphene hydrogenation. **A)** An electrically contacted CVD grown graphene sample is exposed to reactive hydrogen atoms produced by thermal cracking of hydrogen at $T >$1800K in a UHV environment. **B)** The two-point resistance R_{2pt} of the graphene sheet is measured *in situ* with hydrogen dosing. A photograph of the device is shown. **C)** The typical evolution of room temperature resistance versus hydrogen exposure time (circles), and an exponential fit to resistance versus hydrogen dose (dotted line).
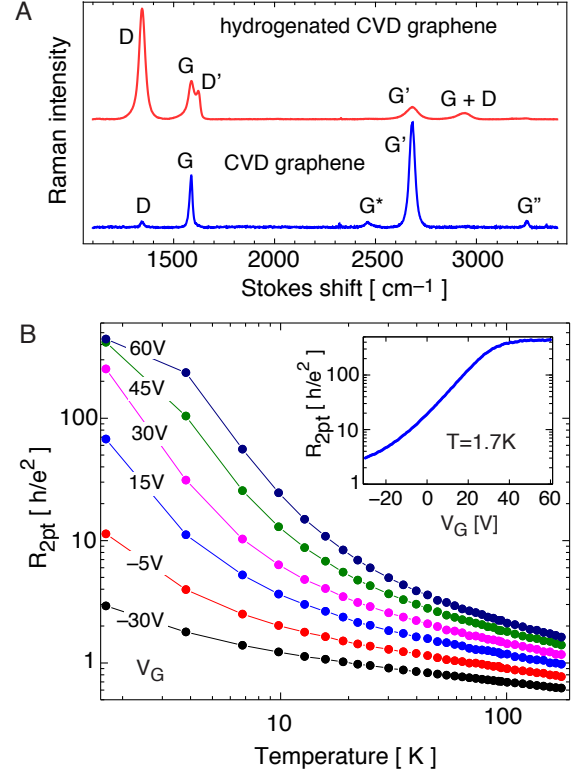

FIG. 2. Characterisation of the hydrogenated graphene devices. **A)** Raman Stokes spectrum of CVD graphene (lower trace) and hydrogenated CVD graphene (higher trace). Peaks associated with sp^2 carbon are classified G, and peaks associated with disorder are classified D, respectively. The ratio I_D/I_G of D peak intensity to G peak intensity is 2.2 and 0.15 for hydrogenated CVD graphene and pristine CVD graphene, respectively, with the corresponding mean defect spacing λ_D estimated to be 4.6 ± 0.5 nm and ~ 35 nm (see text). **B)** The temperature dependence of the resistance is insulating ($dR_{2pt}/dT < 0$) at all gate voltages. The field effect (inset) shows hole conduction and a zero field effect mobility regime at low hole density.

(red spectrum) confirms the introduction of point defects that break the translational invariance of the crystal [14]. The nature of the point defects introduced by hydrogenation is most likely hydrogen-carbon bonds [8]. By direct comparison of the ratio of D peak intensity to G peak intensity, I_D/I_G, with that observed in graphene disordered by controlled ion bombardment [15], we estimate the mean hydrogen-hydrogen spacing to be in the range $\lambda_D \simeq 4.6 \pm 0.5$ nm for a 360s hydrogen exposure, corresponding to a $0.2 - 0.3\%$ hydrogen to carbon ratio.

Electronic transport measurements were performed on the hydrogenated graphene with large ohmic contacts at the opposing corners of a 2.5 mm square using a standard low-frequency technique. The hydrogenated graphene shows unambiguous insulating behaviour, $\partial R_{2pt}/\partial T < 0$, over the entire range of accessible temperatures (from 175K to $\sim$1.7K) and gate induced carrier density, Fig.2**B**. Gate voltage modulation of the resistance shows hole transport with a field effect mobility $\mu = \partial(1/R_{2pt})/\partial(CV_G) \lesssim 10$ cm^2/V$\cdot$s, where the gate capacitance $C = 11.5$ nF/cm^2. A regime of zero field effect mobility is also observed, see inset of Fig.

2**B**, where the Ioffe-Regel parameter is $(k_F\lambda)^{-1} \simeq 700$. In contrast, the Ioffe-Regel parameter in Si [16] and GaAs/AlGaAs [17] where QH and FQH was first observed is $(k_F\lambda)^{-1} \simeq 0.02$. The exponential increase in resistance as $T \to 0$ K appears consistent with a variable-range hopping behaviour $R_0 \exp((T_0/T)^n)$, however we do not find good agreement to either a Mott $n = 1/3$ or Efros-Shklovskii $n = 1/2$ exponent over the temperature range 1.7 K $< T <$ 175 K. Rather, a pronounced saturation in resistance is observed at the lowest hole density and lowest temperatures, corresponding to the emergence of a zero field effect mobility regime of transport.

The 2-point resistance was measured at $T = 575 \pm 25$ mK versus carrier density and in strong magnetic fields, Fig.3**A**. At high hole densities, a colossal negative magnetoresistance is observed from $B = 0$ T through to $B = 45$ T. A similar magnetoresistance was observed

in weakly fluorinated graphene [18]. Conversely, in the regime of zero field effect mobility, the resistance is very weakly dependent on magnetic field below a critical field that is itself dependent upon gate voltage. Remarkably, at a gate voltage $V_G = 21$ V, a sharp transition is observed from an insulating, zero field effect mobility state, to a resistance saturating at a value $R_{2pt} = 12,962$ Ω, which is within 0.5% of $h/2e^2$. In a quantum Hall state, the longitudinal four point resistance $R_{xx} \to 0$ so that the two point resistance approaches the transverse resistance $R_{2pt} \to |R_{xy}|$. The behaviour of R_{2pt} is fully consistent with a Hall component admitting the quantized value $R_{xy} = h/2e^2$. From the known anomalous QH series of graphene $R_{xy} = \pm h/4e^2(N + 1/2)^{-1}$ [2, 3], the hole doping of the sample, and an assumption of preserved spin and valley degeneracies, this QH state corresponds to the $N = -1$ Landau level index and a $\nu = -2$ filling factor. Notably, no Shubnikov-de Haas oscillations in resistance are observed as this QH state is reached at high magnetic field.

The resistance versus gate voltage at constant $B = 45$ T, Fig.3**B**, reveals the charge neutrality point at $V_G = 71 \pm 2$ V between electron and hole conduction. The hole density at $\nu = -2$ required by the magnetic flux density is $2eB/h = 2.17 \times 10^{12}$/cm^2, while the plateau is observed with 3.6×10^{12}/cm^2 holes induced from neutrality. The mobile hole valence band edge is thus located at gate voltage $V_G = 51$ V, providing a signature in electron transport of the formation of a disorder induced gap. Assuming electron-hole symmetry about charge neutrality, we estimate a localized mid-gap state density of 2.9×10^{12}/cm^2. Gap opening and the presence of mid-gap states have been observed in hydrogenated graphene by ARPES [9] and STM [10], with a gap of $\sim 400 - 600$ meV observed for a similar $0.1 - 0.3\%$ hydrogen to carbon ratio. Neither the $\nu = -4$ or $\nu = -6$ plateaus are clearly observed, however the weak resistance minimum at $V_G = -51 \pm 2$ V hints to an emerging $\nu = -6$ QH state. Disorder induced broadening of Landau levels may be responsible for the absence of other plateaus and the absence of Shubnikov-de Haas oscillations.

We plot the emergence of a $\nu = -2$ quantum Hall state at 45 T from a zero-field insulating state versus both the applied magnetic field and the corresponding magnetic length, Fig.3**C**. The magnetic length $\ell_B = \sqrt{\hbar/eB}$ quantifies the magnetic confinement of charge carriers in 2D, independent of material parameters. The insulator-QH transition is here observed with magnetic length spanning $\ell_B = 4 - 6$ nm, consistent with a crossover from weak to tight magnetic confinement with respect to the point defect spacing $\lambda_D = 4.6 \pm 0.5$ nm inferred from Raman spectroscopy. The perspective of an insulator-QH transition arising from magnetic confinement of charge carriers below the mean defect spacing is complementary to the picture of extended states floating in energy that
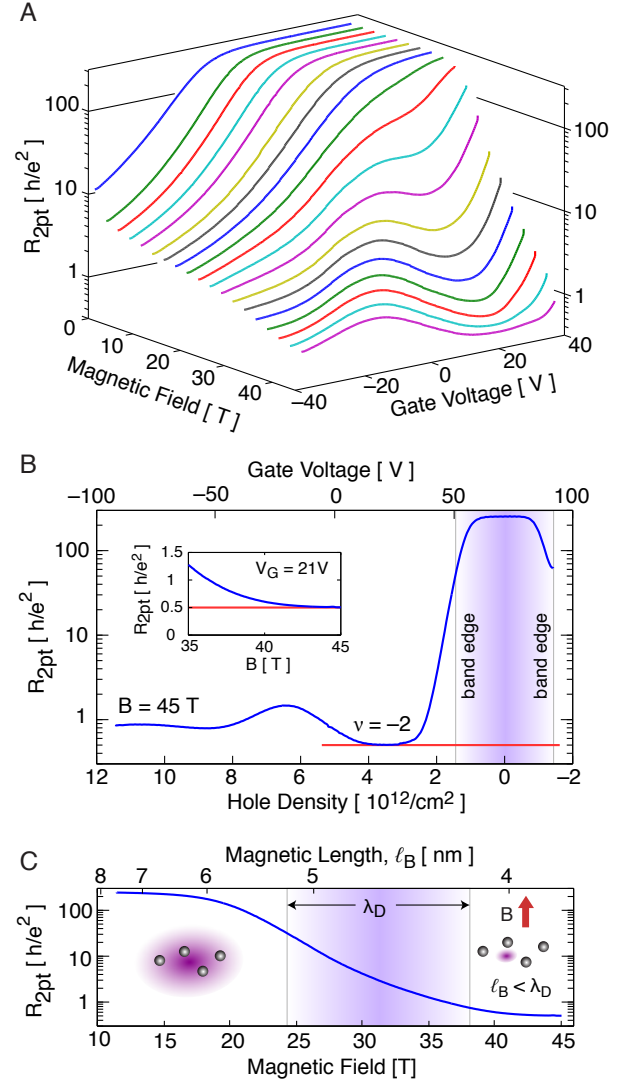

FIG. 3. Quantum Hall effect in hydrogenated graphene. **A)** The two-point resistance of the hydrogenated graphene sheet is shown versus the magnetic field and the gate voltage. The resistance axis is shown on a logarithmic scale, in units of the resistance quantum $R_q = h/e^2$. All data were taken at a temperature of 575 ± 25 mK. **B)** At 45T, the resistance versus gate voltage (upper x-axis) and hole density (lower x-axis), with the red line indicating a Hall plateau at $R = h/2e^2$. The inset shows the resistance at 21V gate voltage approach the quantum Hall state plateau with increasing magnetic field. **C)** Resistance of the hydrogenated graphene at 21V gate voltage plotted versus both the magnetic field (lower x-axis) and magnetic length ℓ_B (upper x-axis). The shaded region indicates the estimated point defect spacing extracted from the Raman spectra.

has been previously used to explain insulator-QH transitions [19]. Further work is required to elucidate the role of length scales in the insulator-QH transition, in particular the interplay between the magnetic length, mean defect spacing, and electron density.
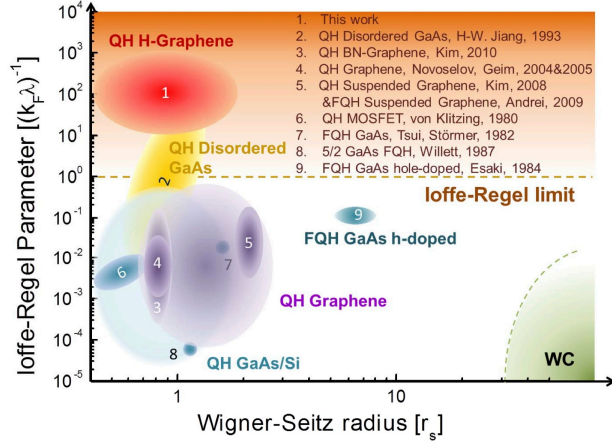
giving $\Delta E_{0\to\pm1} = 240$ meV at 45 T. Previous reports of ARPES of graphene hydrogenated to a $0.1 - 0.3$ % hydrogen-carbon ratio gives an estimated zero-field gap of $E_G \sim 400 - 600$ meV [9]. In comparison, the bandgap of GaAs, the choice material for high mobility 2DEGs, is ~ 1.5 eV which is $\sim 20\times$ larger than the cyclotron energy $\hbar eB/m* = 78$ meV separating Landau levels at 45 T. We propose that the energy scales experimentally accessible in hydrogenated graphene enable the study of the competition between disorder and magnetic confinement, leading to new understanding of the role of disorder in the QHE.

Acknowledgments

FIG. 4. 'Ioffe-Regel' - 'Wigner-Seitz' diagram for the main families of materials exhibiting the quantum Hall effect. The figure shows the zero-field value of the Ioffe-Regel disorder parameter $(k_F\lambda)^{-1}$ plotted versus the Wigner-Seitz radius r_s, both dimensionless, for the main 2DEG families in which the integer and fractional quantum Hall effect was observed. A brief description of the material system, indexed numerically, is given in the upper right. The size of the labeled regions is representative of the parameter range from observed mobilities and densities. The dashed line shows the Ioffe-Regel limit where $k_F\lambda = 1$. The Wigner crystal (WC), thought to occur at large r_s and low disorder, is highlighted in green.

The emergence of a quantum Hall state from a zero field effect mobility insulating state raises the question of how much disorder can be introduced into a 2D electron gas (2DEG) and still form a quantum Hall state. A diagram summarizing 2DEG systems where the quantum Hall effect (QHE) has been observed is plotted in Fig.4 versus the dimensionless Ioffe-Regel disorder parameter $(k_F\lambda)^{-1}$, with λ the transport mean free path, and the dimensionless Wigner-Seitz radius r_S quantifying interaction strength. The preponderance of 2DEGs where the QHE has been observed are low-disorder samples satisfying the Ioffe-Regel criterion (in zero magnetic field) $(k_F\lambda)^{-1} \ll 1$. However, a previous study in disordered GaAs/AlGaAs heterostructures biased to subthreshold conditions exhibited strong disorder $(k_F\lambda)^{-1} > 1$ at low carrier density and a transition from localization to a QH state[20]. Our observations with hydrogenated graphene pushes the limit of disorder to $(k_F\lambda)^{-1} \gtrsim 500$ where the QHE can still be attained in a strong magnetic field, suggesting that the QHE might be robust to arbitrarily large disorder.

The insulator-QH transition in hydrogenated graphene opens a new regime in energy scales previously unavailable to experiments. The Landau level energy gap about the $N = 0$ Landau level is $\Delta E_{0\to\pm1} = \sqrt{2}\hbar v_F/\ell_B$ [3],

[1] K.S. Novoselov *et al.*, *Science* **306**, 696 (2004).
[2] K.S. Novoselov *et al.*, *Nature* **438**, 197 (2005).
[3] Y. Zhang, Y.-W. Tan, H.L. Störmer, and P. Kim, *Nature* **438**, 201 (2005).
[4] Y. Zhang *et al.*, *Phys. Rev. Lett.* **96**, 136806 (2005).
[5] A.F. Young *et al.*, *Nat. Physics* **8**, 550 (2012).
[6] X. Du, I. Skachko, F. Duerr, A. Luican, and E.Y. Andrei, *Nature* **462**, 192 (2009).
[7] C.R. Dean *et al.*, *Nat. Physics* **7**, 693 (2011).
[8] D.C. Elias *et al.*, *Science* **323**, 610 (2009).
[9] D. Haberer *et al.*, *Nano Lett.* **10**, 3360 (2010).
[10] D. Haberer *et al.*, *ACS Nano*, in print (2012).
[11] X.S. Li *et al. Science* **324**, 1312 (2009).
[12] A. Guermoune *et al.*, *Carbon* **49**, 4204 (2011).
[13] U. Bischler and E. Bertel, *J. Vac. Sci. Tech. A* **11**, 458 (1993).
[14] A. Jorio *et al.*, *Raman Spectroscopy in Graphene Related Systems*, Wiley-VCH, Singapore, 2011.
[15] M.M. Lucchese *et al.*, *Carbon* **48**, 1592 (2010).
[16] K. von Klitzing, G. Dorda, and M. Pepper, *Phys. Rev. Lett.* **45**, 494 (1980).
[17] D.C. Tsui, H.L. Störmer, and A.C. Gossard, *Phys. Rev. Lett.* **48**, 1559 (1982).
[18] X. Hong *et al.*, *Phys. Rev. B* **83**, 085410 (2011).
[19] S. Das Sarma and A. Pinczuk, Eds, *Perspectives in Quantum Hall Effects: Novel Quantum Liquids in Low-Dimensional Semiconductor Structures*, p. 23, Wiley-VCH, Singapore, 1996.
[20] H.-W. Jiang *et al.*, *Phys. Rev. Lett.* **71**, 1439 (1993).